ments will both extend the energy range of the spin assignments in $^{235}U+n$ and decrease the number of unassigned resonances in the range discussed here.

†Work performed under the auspices of the U. S. Atomic Energy Commission.

[1]R. I. Schermer, L. Passell, G. Brunhart, C. A. Reynolds, V. L. Sailor, and F. J. Shore, Phys. Rev. 167, 1121 (1968).

[2]E. R. Reddingius, H. Postma, C. E. Olsen, D. C. Rorer, and V. L. Sailor, "Spins of Low Energy Neutron Resonances in ^{235}U" (to be published).

[3]G. A. Keyworth, J. R. Lemley, C. E. Olsen, F. T. Seibel, J. W. T. Dabbs, and N. W. Hill, "Spin Determination of Intermediate Structure in the Subthreshold Fission of ^{237}Np" (to be published).

[4]G. K. Shenoy, M. Kuznietz, B. D. Dunlap, and G. M. Kalvius, Phys. Lett. 42A, 61 (1972).

[5]F. Corvi, M. Stefanon, C. Coceva, and P. Giacobbe, Nucl. Phys. A203, 145 (1973).

[6]R. G. Graves, R. E. Chrien, D. J. Garber, G. W. Cole, and O. A. Wasson, Phys. Rev. C 8, 787 (1973).

[7]H. Weigmann, J. Winter, and M. Heske, Nucl. Phys. A134, 535 (1969).

[8]W. R. Kane, Phys. Rev. Lett. 25, 953 (1970).

[9]M. Asghar, A. Michaudon, and D. Paya, Phys. Lett. 26B, 664 (1968).

[10]F. Poortmans, H. Ceulemans, E. Migneco, and J. Theobald, in *Proceedings of the Second International Conference on Nuclear Data for Reactors, Helsinki, Finland, 1970* (International Atomic Energy Agency, Vienna, Austria, 1970), p. 449.

[11]F. B. Simpson, L. G. Miller, and M. S. Moore, Nucl. Phys. A164, 34 (1971).

[12]G. A. Cowan, B. P. Bayhurst, and R. J. Prestwood, Phys. Rev. 130, 2380 (1963).

[13]G. A. Cowan, B. P. Bayhurst, R. J. Prestwood, J. S. Gilmore, and G. W. Knobeloch, Phys. Rev. C 2, 615 (1970).

[14]G. De Saussure, R. B. Perez, and W. Kolar, Phys. Rev. C 7, 2018 (1973).

[15]N. J. Pattenden and H. Postma, Nucl. Phys. A176, 225 (1971).

[16]J. W. T. Dabbs, C. Eggerman, B. Cauvin, A. Michaudon, and M. Sanche, in *Proceedings of the Second International Atomic Energy Symposium on Physics and Chemistry of Fission, Vienna, Austria, 1969* (International Atomic Energy Agency, Vienna, Austria, 1969), p. 321.

[17]F. Poortmans, H. Ceulemans, J. Theobald, and E. Migneco, in *Proceedings of the Third Conference on Neutron Cross Sections and Technology, Knoxville, Tennessee, 1971,* edited by R. Macklin, CONF-710301 (U.S. AEC Division of Technical Information, Oak Ridge, Tenn., 1971), Vol. 2, p. 667.

Characteristics of the Reaction $p + p \rightarrow p + X$ at 205 GeV/c*

S. J. Barish, D. C. Colley,† and P. F. Schultz
Argonne National Laboratory, Argonne, Illinois 60439

and

J. Whitmore
National Accelerator Laboratory, Batavia, Illinois 60510

(Received 6 August 1973)

The inelastic reaction $p+p \rightarrow p+X$ is studied at 205 GeV/c. The distribution of the square of the missing mass, M^2, shows a large diffractivelike peak at low M^2 due to two-, four-, and six-prong events. The slope of the invariant cross section versus t decreases with increasing M^2. The energy dependences of the multiplicity moments for the recoiling system X are similar to those for corresponding moments for $p+p \rightarrow (n$ charged particles).

The existence of excited states of the proton has been established by experiments at beam momenta below ~30 GeV/c. Some of these states with low mass have been found to be produced diffractively, i.e., with approximately energy-independent cross sections, and therefore are also expected to occur at higher energies. In this Letter we present results on the inelastic reaction $p+p \rightarrow$ (slow p) $+X$ obtained using data from a 50 000-picture exposure of the 30-in. liquid-hydrogen bubble chamber to a beam of 205-GeV/c protons at the National Accelerator Laboratory. The objectives of our analysis were to study the diffractivelike excitation of the beam proton by examining the distribution of the square of the missing mass, M^2, recoiling against the slow proton, and to investigate the characteristics of the process. Data at 102[1] and 303 GeV/c[2] and

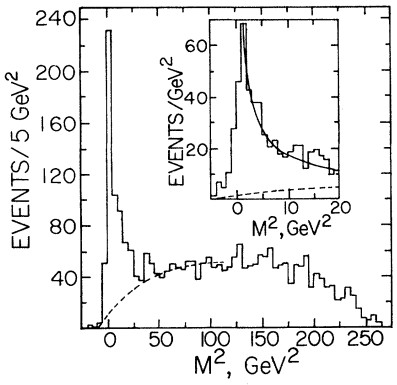

FIG. 1. Weighted distribution in the square of the missing mass, M^2, for inelastic events of the type $p+p \rightarrow (\text{slow } p)+X$. The inset shows the low-M^2 region in 1-GeV^2 bins. The dashed lines represent a hand-drawn background used to estimate the number of events in the peak. The solid curve on the inset shows background plus a $1/M^2$ dependence for the tail of the peak.

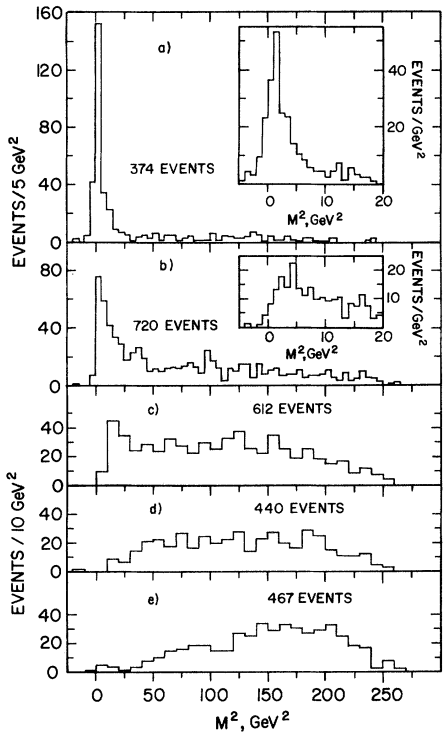

FIG. 2. Weighted M^2 distributions for (a) inelastic two-prong, (b) four-prong, (c) six-prong, (d) eight-prong, and (e) greater than eight-prong events. Insets in (a) and (b) show the low-M^2 region in 1-GeV^2 bins.

at intersecting-storage-rings energies[3] show peaks at low M^2, but the dependence of peak position on charged-particle multiplicity and the behavior of t distributions as a function of M^2 have not been studied in detail (t is the square of the four-momentum transfer from target to recoil proton).

The results reported here are based on 3600 events having protons with lab momentum less than 1.4 GeV/c. We have applied to the data appropriate weights (ranging from 1.04 to 1.17 for different topologies) to compensate for scanning and processing losses.[4] To obtain distributions for inelastic events only, we have subtracted the elastic events which form the majority of the two-prong events. All two-prong events in the exposure have been measured completely and kinematically fitted.[5] Removal of the 1100 events that give an elastic fit[6] and the 200 that have not been measured well enough for a three- or four-constraint fit to be attempted leaves 300 ± 40 inelastic two-prong events (before weighting).

The M^2 distribution for all events (which is unbiased by our slow-proton selection up to $M^2 = 150$ GeV^2) is given in Fig. 1. It shows a striking peak below 5 GeV^2, with a tail extending above 25 GeV^2. After allowing for background, the shape of the tail is consistent with a falloff of the approximate form $1/M^2$ expected for a triple-Pomeron process (see curves on the inset in Fig. 1). Plots for the different charged multiplicities contributing to the sample are given in Fig. 2 and show that the peak in the distribution for all events comes mainly from the two- and four-prong events, with a small contribution from the six-prong events. A noticeable feature of these plots is that the peak position moves up in M^2 from below 2 GeV^2 for the two-prong events, to ~4 GeV^2 for the four-prong events [see the insets in Figs. 2(a) and 2(b)], and to ~16 GeV^2 for the six-prong events. There are no significant peaks in the distributions for events with eight or more prongs.

We take the existence of the peak in Fig. 1 as a clear indication of the presence of diffractive fragmentation leading to states with low M^2 and low multiplicity. The cross section for events above background in the peak has been calculated (using a microbarn equivalent for our data of 4.35 ± 0.1 μb/event) to be $\sigma_s = 2.6 \pm 0.3$ mb.[7] This represents a lower limit on the cross section for diffractive fragmentation of the beam proton, since we have no way of estimating any contributions from diffractive processes leading to high-M^2 states or yielding distributions that do not peak at low M^2. We estimate that $(44 \pm 6)\%$ of σ_s is due to the two-prong, $(46 \pm 5)\%$ to the four-prong, and $(10 \pm 3)\%$ to the six-prong events. As-

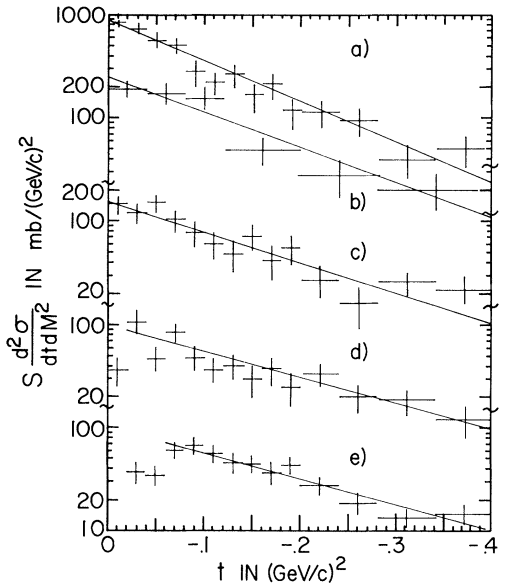

FIG. 3. Invariant cross section $s\,d^2\sigma/dt\,d(M^2)$ versus the square of the four-momentum transfer, t, for all events for (a) $M^2 < 5$ GeV^2, (b) $5 \leq M^2 < 10$ GeV^2, (c) $10 \leq M^2 < 25$ GeV^2, (d) $25 \leq M^2 < 50$ GeV^2, and (e) $50 \leq M^2 < 100$ GeV^2. The lines drawn show fits of the form Ae^{Bt} to the data (see Table I).

suming factorization for whatever processes contribute to the peak, the double diffractive cross section $\sigma_d = \sigma_s^2/\sigma_{el} = 1.0 \pm 0.2$ mb (using 6.8 ± 0.2 mb for σ_{el}, the elastic pp cross section), so that a lower limit on the total diffractive cross section for beam, target, or both protons is 6.2 ± 0.7 mb at 205 GeV/c. Values quoted at other energies (though each experiment uses a different method of estimating σ_s) are 8.5 ± 1.5 mb at 102 GeV/c[1] and 6.8 ± 1.0 mb at 303 GeV/c.[2]

To show the behavior of the slow-proton events as a function of four-momentum transfer, we give in Fig. 3 plots of $s\,d^2\sigma/dt\,d(M^2)$ for several ranges of M^2. The t dependence of each distribution can be well fitted by the form Ae^{Bt}, except in those bins affected by the kinematic boundary at high values of M^2. Even though we have made no corrections for loss of protons with $-t \lesssim 0.01$ (GeV/c)^2 in the two-prong events, where such a loss is likely to occur, the t distributions for $M^2 < 50$ GeV^2 do not show any falloff as $t \to 0$. Thus, if the low-M^2 peak were due to a triple-Pomeron process, our data indicate a nonzero value for the coupling at the triple-Pomeron vertex even at $t \simeq -0.01$ (GeV/c)^2.

We have also fitted the distributions for two-, four-, six-, and eight-prong events separately. The values of B obtained in all the fits are given in Table I. Within statistics, all topologies have similar values of B for each M^2 range. Below $M^2 = 5$ GeV^2, the slope parameters are near the value of 11 ± 1 (GeV/c)$^{-2}$ found for elastic pp scattering,[8] but at higher M^2 the values are significantly lower. We note that even within the low-M^2 peak ($M^2 < 25$ GeV^2), there is a substantial decrease in B as M^2 increases.

Finally, we show in Fig. 4(a) the average multiplicity $\langle n_{M^2} \rangle$ for the charged particles recoiling against the slow proton as a function of M^2, the square of the mass of the recoiling system. We also include data from the 102- and 303-GeV/c experiments. These agree well with our results, showing that there is no strong dependence on beam energy over the range considered. We also show in Fig. 4(a) a curve obtained by fitting the s dependence of the average charged-particle multiplicity for real inelastic pp collisions [i.e., $p + p \to (n$ charged particles)]. The form used for the fit[9] was $\langle n \rangle = A + B \ln s + C/\sqrt{s}$, and we have plotted $\langle n_{M^2} \rangle = A + B \ln(M^2) + C/\sqrt{M^2}$ with the same values of the coefficients found in the fit ($A = -4.8$, $B = 2$, $C = 10$). Though our data lie systematically above this curve, they show a remarkably similar energy dependence. We have also examined other moments of the multiplicity distributions for the recoil system as a function of M^2. Figures 4(b)–4(d) show, respectively, $f_2 = \langle n_{M^2}(n_{M^2} - 1) \rangle - \langle n_{M^2} \rangle^2$, $\langle n_{M^2}^{-} \rangle$, and f_2^{-} plotted versus M^2. Each of these shows an energy dependence very much like that for the corresponding quantity for

TABLE I. Values of B in (GeV/c)$^{-2}$ obtained by fitting $d\sigma/dt$ to Ae^{Bt}.

M^2 (GeV^2)	t [(GeV/c)^2]	All events	Two-prong events	Four-prong events	Six-prong events	Eight-prong events
< 5	0.0 −0.4	9.1 ± 0.7	8.7 ± 0.8	10.2 ± 1.5	···	···
5– 10	0.0 −0.4	8.0 ± 1.1	···	8.4 ± 1.6	···	···
10– 25	0.0 −0.4	6.1 ± 0.7	···	6.2 ± 1.1	8.6 ± 1.5	···
25– 50	0.02–0.4	5.8 ± 0.7	···	5.1 ± 1.3	5.2 ± 1.3	6.4 ± 1.7
50–100	0.06–0.4	5.8 ± 0.6	···	7.6 ± 1.5	3.5 ± 1.1	4.8 ± 1.3

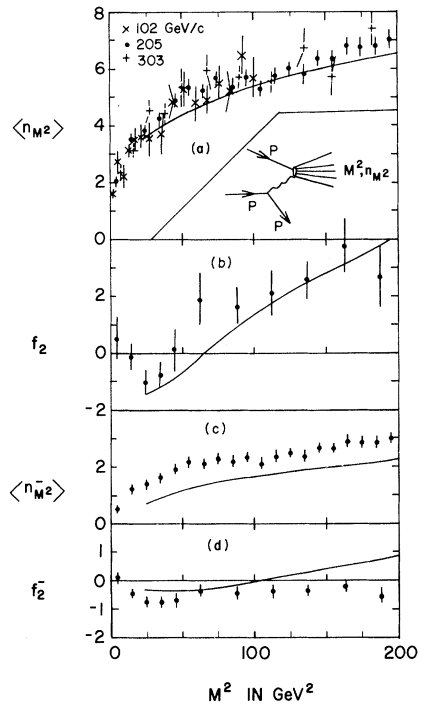

FIG. 4. Moments of the charged system X recoiling against the slow proton in $p+p \to (\text{slow } p)+X$ plotted versus M^2, the square of the mass of X. (a) $\langle n_{M^2} \rangle$, (b) $f_2 = \langle n_{M^2}(n_{M^2}-1) \rangle - \langle n_{M^2} \rangle^2$, (c) $\langle n_{M^2}^- \rangle$, and (d) f_2^-. The curve in (a) shows $\langle n \rangle = -4.8 + 2\ln(M^2) + 10/\sqrt{M^2}$, where the coefficients are taken from a fit (Ref. 9) of $\langle n \rangle$ versus c.m. energy for real pp interactions, $p+p \to (n$ charged particles). The curves in (b)–(d) show the dependences on s of f_2, $\langle n^- \rangle$, and f_2^- for real pp collisions.

real pp collisions (shown by the curves in the diagrams).

If the reaction $p+p \to p+X$ proceeds by exchange of a single particle that excites the beam proton [as shown by the inset in Fig. 4(a)], then studying the properties of the recoil system as a function of M^2 is equivalent to studying the interaction of the exchanged particle with a proton as a function of s. Assuming this picture is correct,[10] then the agreement between our data and the real pp results shows that exchange-particle–proton interactions are strikingly similar in character to real pp collisions.

We are grateful to the National Accelerator Laboratory staff for assistance in obtaining the film, and to measuring and scanning personnel at Argonne National Laboratory and the State University of New York at Stony Brook. We are indebted to H. Yuta for work on the two-prong events, and we acknowledge useful discussions with J. Dash and D. Snider. We also wish to thank T. Fields for many useful comments and suggestions.

---

*Work supported by the U.S. Atomic Energy Commission.

†On leave from the University of Birmingham, Birmingham, England.

[1]C. M. Bromberg *et al.*, University of Rochester and University of Michigan Report No. UR416/UMBC 72-14 (to be published).

[2]F. T. Dao *et al.*, Phys. Lett. 45B, 399, 402 (1973).

[3]M. G. Albrow *et al.*, Nucl. Phys. B54, 6 (1973).

[4]Details of these corrections will be given in another publication.

[5]S. Barish *et al.*, ANL Report No. ANL/HEP 7337 (to be published). The observed width in M^2 for the elastic events agrees with the resolution in M^2 of ± 1.5 GeV^2 estimated using kinematic variables.

[6]Since this procedure is subject to considerable uncertainty, we have assigned an error of ± 35 to the 156 inelastic two-prong events with $M^2 < 5$ GeV^2, where the inelastics and elastics overlap. We have verified that the shape of the inelastic two-prong M^2 distribution is not sensitive to small variations in the method used for selecting elastic fits.

[7]There are 850 ± 50 events below $M^2 = 50$ GeV^2, and we have taken the background as 260 ± 50 events.

[8]V. Bartenev *et al.*, Phys. Rev. Lett. 29, 1755 (1972).

[9]D. M. Tow, Phys. Rev. D 7, 3535 (1973).

[10]It is important to note that only for low M^2 ($\lesssim 25$ GeV^2) is Pomeron exchange likely to be the dominant contribution to the process suggested in Fig. 4(a).